

Factors Influencing the DNA Nuclease Activity of Iron, Cobalt, Nickel, and Copper Chelates

Jeff C. Joyner,^{†,‡} Jared Reichfield,[†] and J. A. Cowan^{*,†,‡,§}

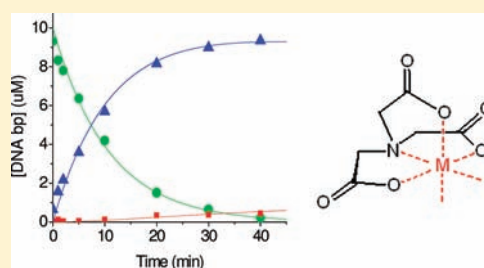
[†]Evans Laboratory of Chemistry, The Ohio State University, 100 West 18th Avenue, Columbus, Ohio 43210, United States

[‡]The Ohio State Biochemistry Program, 784 Biological Sciences, 484 West 12th Avenue, Columbus, Ohio 43210, United States

[§]MetalloPharm LLC, 1790 Riverstone Drive, Delaware, Ohio 43015, United States

S Supporting Information

ABSTRACT: A library of complexes that included iron, cobalt, nickel, and copper chelates of cyclam, cyclen, DOTA, DTPA, EDTA, tripeptide GGH, tetrapeptide KGHK, NTA, and TACN was evaluated for DNA nuclease activity, ascorbate consumption, superoxide and hydroxyl radical generation, and reduction potential under physiologically relevant conditions. Plasmid DNA cleavage rates demonstrated by combinations of each complex and biological co-reactants were quantified by gel electrophoresis, yielding second-order rate constants for DNA_{supercoiled} to DNA_{nicked} conversion up to $2.5 \times 10^6 \text{ M}^{-1} \text{ min}^{-1}$, and for DNA_{nicked} to DNA_{linear} up to $7 \times 10^5 \text{ M}^{-1} \text{ min}^{-1}$. Relative rates of radical generation and characterization of radical species were determined by reaction with the fluorescent radical probes TEMPO-9-AC and rhodamine B. Ascorbate turnover rate constants ranging from 3×10^{-4} to 0.13 min^{-1} were determined, although many complexes demonstrated no measurable activity. Inhibition and Freifelder–Trumbo analysis of DNA cleavage supported concerted cleavage of dsDNA by a metal-associated reactive oxygen species (ROS) in the case of $\text{Cu}^{2+}(\text{aq})$, Cu-KGHK, Co-KGHK, and Cu-NTA and stepwise cleavage for $\text{Fe}^{2+}(\text{aq})$, Cu-cyclam, Cu-cyclen, Co-cyclen, Cu-EDTA, Ni-EDTA, Co-EDTA, Cu-GGH, and Co-NTA. Reduction potentials varied over the range from -362 to $+1111 \text{ mV}$ versus NHE, and complexes demonstrated optimal catalytic activity in the range of the physiological redox co-reactants ascorbate and peroxide (-66 to $+380 \text{ mV}$).



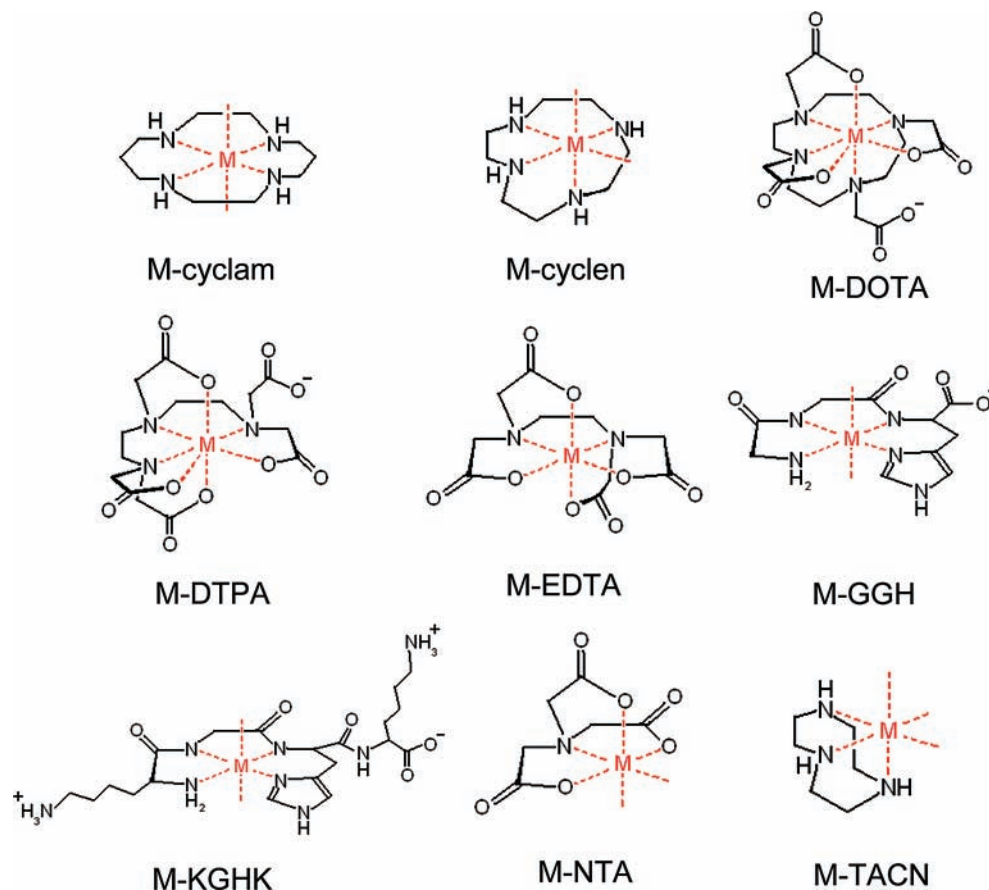
INTRODUCTION

There is significant interest in the development of artificial nucleases, especially those that cause sequence-specific inactivation of disease-associated genes. Because diseases such as cancer and AIDS ultimately stem from genetic sources, they require a gene modification strategy at the DNA level, rather than downstream products, to effect a cure. Current anti-cancer strategies include the use of DNA-binding cisplatin derivatives,^{1,2} DNA intercalators,^{3,4} and alkylating drugs^{5,6} as anti-neoplastic agents. Progress in gene therapy has been unsatisfactory, since even the most successful attempts tend to result in secondary cancers as a result of unintended insertional mutagenesis.^{7,8} Another important approach for anti-cancer and anti-HIV therapy is the use of compounds that incorporate both a DNA-damaging hydrolytic or redox-active metal complex and a stable gene-specific targeting sequence, such that the compound can both specifically hybridize to and damage the targeted disease-associated gene, leaving other genes unaffected.^{9–14} In addition to gene targeting and cell delivery, two major factors critical to the success of redox-dependent DNA-targeting compounds are their abilities to efficiently utilize biologically available redox co-reactants, as required, and to function with multiple turnovers.^{15–19} Artificial nucleases must be very efficient in order to compete with the innate cellular DNA repair machinery.

With these factors in mind, our goal in this study was to determine and compare the DNA nuclease activities, oxidative pathways, and reduction potentials of various metal-chelate complexes that are likely candidates for incorporation into gene-specific artificial nucleases. These studies also served to elucidate the factors required for optimal nuclease activity, as well as to identify several metal-chelates with many, if not all, of the desired properties for use in gene-selective nuclease catalysts. A library consisting of combinations of the transition metals Fe^{2+} , Co^{2+} , Ni^{2+} , and Cu^{2+} with the chelators cyclam, cyclen, DOTA, DTPA, EDTA, tripeptide GGH, tetrapeptide KGHK, NTA, and TACN was studied (Scheme 1). These ligands reflect the broad range of carboxylate and cyclic amine chelates that commonly form the basic framework for DNA cleavage agents, and also build on our prior studies of the natural ATCUN peptide sequence.^{16–18,20,21} DNA cleavage rates, co-reactant consumption rates, radical generation rates, characterization of reactive intermediates, co-reactant selectivity, and reduction potentials were determined. As expected, the chelators were found to significantly modulate the behavior of these transition metals, resulting in a wide variety of nuclease activity, observed mechanisms, and reduction potentials.

Received: June 7, 2011

Published: August 04, 2011

Scheme 1. Summary of the Metal-Chelates Used in This Study ($M = \text{Fe}^{2+}$, Co^{2+} , Ni^{2+} , or Cu^{2+})^a

^a These complexes are expected to accommodate up to a six-coordinate metal coordination geometry, although Fe-DOTA and Fe-DTPA have typically been shown to adapt a seven-coordinate metal coordination geometry. The M-cyclam and ATCUN (GGH and KGHK) complexes tend to leave two trans open coordination sites, while M-cyclen complexes have two cis open coordination sites as a result of the smaller chelate size relative to the metal. Finally, M-TACN complexes have three open coordination sites.^{22,31–37}

Reactivity was also highly dependent on the available redox co-reactants.

These results are useful for interpretation of the metal-mediated mechanisms responsible for the observed DNA nuclease activities. While many of the metal complexes studied herein have been the focus of prior reports,^{12,18,20,22–30} comparison of data is hindered by the range of experimental conditions used. Moreover, a variety of mechanisms and rates of DNA cleavage have been reported, reflecting variations of solution pH and buffers and the use of solution co-reactants of varying redox potentials, all of which preclude an accurate comparison of the reactivity of these metal complexes. The studies reported here were conducted under uniform conditions, allowing a high degree of confidence when making comparisons between metal-chelates or assays. The results obtained and conclusions drawn should provide a benchmark for future work in this area.

MATERIALS AND METHODS

Chemicals and Reagents. The chelators 1,4,7,10-tetraazacyclododecane (cyclen) and 1,4,7,10-tetraazacyclododecane-1,4,7,10-tetraacetic acid (DOTA) were obtained from Macrocylics. Tripeptide GGH-OH (GGH) and tetrapeptide KGHK-OH (KGHK) were obtained from Bachem. 1,4,8,11-Tetraazacyclotetradecane (cyclam), diethylenetri-

minepentaacetic acid (DTPA), nitrilotriacetic acid (NTA), and 1,4,7-triazacyclononane (TACN) were purchased from Sigma. Ethylenediaminetetraacetic acid (EDTA) was purchased from Aldrich. Fe(II) sulfate heptahydrate, Co(II) chloride hexahydrate, Ni(II) tetrahydrate, and Cu(II) chloride dihydrate were purchased from ACROS, J.T. Baker, Aldrich, and J.T. Baker, respectively. Salts, NaCl and NaOH, were purchased from Fisher, and HEPES was purchased from Sigma. Ascorbic acid and rhodamine B were purchased from Fluka. Stabilized 30% hydrogen peroxide solution and dibasic sodium phosphate were purchased from Sigma-Aldrich. TEMPO-9-AC was purchased from Invitrogen.

Sample Handling and Preparation. The water used in all procedures was purified using a Barnstead NANOpure Diamond filtration system with a 0.2 μm pore size filter. Plasmid DNA was isolated from a pUC19 transformed DH5 α *Escherichia coli* cell line and purified by use of a Qiagen miniprep kit following water elution from spin columns (the use of EDTA-containing buffer was avoided). The isolated DNA was quantified by absorbance measurements, divided into single-use aliquots in water, and frozen at -20 °C. Ascorbic acid solutions were prepared freshly each day by making a 100 mM ascorbic acid solution in 20 mM HEPES, 100 mM NaCl, and balancing the pH to 7.4 with 1 M NaOH. Ascorbic acid was kept on ice and diluted prior to each experiment. Solutions of H_2O_2 were made and used in a similar manner, but without the subsequent pH balancing, since the H_2O_2 concentrations used did not alter the pH of the buffer. Stock H_2O_2 solutions were freshly prepared from a refrigerated 30% H_2O_2 stock and

maintained on ice prior to use. The TEMPO-9-AC radical probe was initially dissolved in DMSO and diluted into aliquots in 20 mM HEPES, 100 mM NaCl, pH 7.4. Metal-chelate (M-chelate) complexes were prepared freshly on the day of use by mixing the respective metal salt solution in water with the chelator in buffer to a final ratio of 1:1.5 and incubating for 20–30 min at room temperature. A slight excess of chelator was added to ensure that no free metal ion was present. Complex formation and chelator concentration were verified by UV/vis titration. As expected,¹⁷ Fe²⁺ did not form stable complexes with either GGH or KGHK, while complex formation between iron and the chelators cyclam and cyclen was not observed under the conditions used in these studies (20 mM HEPES, 100 mM NaCl, pH 7.4). Accordingly, these four complexes were not included in the assays described herein.

Gel Electrophoresis Analysis of Plasmid DNA Cleavage.

Reactions were run aerobically with 10 μ M base pair pUC19, 100 nM M-chelate, 1 mM H₂O₂, and 1 mM ascorbate in 20 mM HEPES, 100 mM NaCl, pH 7.4. For each M-chelate, eight time points were collected by incubating eight tubes in parallel, initiating reaction at staggered time points over 6 h, and quenching simultaneously by placing on ice and adding loading dye. The quenched reactions were immediately loaded onto 1% agarose gels containing ethidium bromide, separated for 30–45 min at 120 V, and visualized using a BioRad gel doc. Supercoiled, nicked, and linearized plasmid DNA at each time point was quantified with the program ImageQuant. A correction factor of 1.47 was applied for the intensity of supercoiled DNA to account for the diminished ability of supercoiled DNA to intercalate ethidium bromide.¹⁸ Time-dependent supercoiled, nicked, and linear DNA concentration data were fit to a first-order consecutive model defined by eqs 1, 2, and 3, where *S*, *N*, and *L* correspond to the concentrations of supercoiled, nicked, and linearized plasmid, respectively, *S*₀, *N*₀, and *L*₀ correspond to the respective initial concentrations, and *k*_{nick} and *k*_{lin} correspond to the observed first-order rate constants of DNA nicking and linearization, respectively. Observed rate constants were expressed as min⁻¹. DMSO inhibition of DNA cleavage by each M-chelate was performed as described, with the exception that only 30 min time points were used for each M-chelate with variable concentrations of DMSO (0, 10, 100, 1000 mM), and IC₅₀ values were determined.

$$S = S_0 \exp(-k_{\text{nick}}t) \quad (1)$$

$$N = S_0[k_{\text{nick}}/(k_{\text{lin}} - k_{\text{nick}})]\{\exp(-k_{\text{nick}}t) - \exp(-k_{\text{lin}}t)\} + N_0 \exp(-k_{\text{lin}}t) \quad (2)$$

$$L = S_0\{1 + [k_{\text{nick}} \exp(-k_{\text{lin}}t) - k_{\text{lin}} \exp(-k_{\text{nick}}t)]/(k_{\text{lin}} - k_{\text{nick}})\} + N_0[1 - \exp(-k_{\text{lin}}t)] + L_0 \quad (3)$$

Freifelder–Trumbo Analysis of DNA Linearization.

Freifelder–Trumbo analysis was performed as described previously.^{18,38} Briefly, the fractions of full-length linear (*f*_{lin}) and supercoiled (*f*_{super}) DNA remaining at the individual time points in the electrophoresis gels used to monitor M-chelate/DNA reactions were determined. The fractions at that time are statistically related to the probable number of double strand breaks (*n*₂) and single strand breaks (*n*₁) by the simplified Poisson distribution defined by eq 4, and the Freifelder–Trumbo relation defined by eq 5. These fractions (*f*_{lin} and *f*_{super}), and eqs 4 and 5, were used simultaneously to solve for *n*₂/*n*₁ ratios for each M-chelate. The *n*₂/*n*₁ ratios were then used to assess whether DNA linearization by each M-chelate occurred by a concerted mechanism or random nicking, as described.

$$f_{\text{lin}} = n_2 \exp(-n_2) \quad (4)$$

$$f_{\text{super}} = \exp[-(n_1 + n_2)] \quad (5)$$

Determination of Overall Diffusible Radical Generation by TEMPO-9-AC Fluorescence.

Reactions were run aerobically with 10 μ M TEMPO-9-AC and 10 μ M M-chelate, with and without 1 mM H₂O₂, in 20 mM HEPES, 100 mM NaCl, pH 7.4, in a black-wall 96-well plate. The increase of TEMPO-9-AC fluorescence upon reaction was monitored in real time by excitation at 358 nm and emission at 435 nm every 4 min on a Varian Cary Eclipse fluorimeter with plate reader attachment. The overall change in fluorescence, which corresponded to the complete reaction of 10 μ M TEMPO-9-AC, was used to convert units of fluorescence intensity into units of μ M TEMPO-9-AC, and the rates of reaction (μ M TEMPO-9-AC/min) were determined from the slopes of the kinetic plots of fluorescence intensity versus time. The Fe-TACN/H₂O₂/TEMPO reaction was monitored by stopped-flow techniques due to the extremely high rate. Stopped-flow measurements were made using an Applied Photophysics SpectraKinetic monochromator, with excitation at 358 nm and an emission filter with band-pass > 395 nm. Two syringes were used, one containing 20 μ M TEMPO-9-AC and 2 mM H₂O₂, and the other containing 20 μ M Fe-TACN. Data were collected only after two purge injections, and the fitted kinetic trace for the Fe-TACN/H₂O₂/TEMPO reaction was the average of five trials.

Determination of Hydroxyl Radical Generation by Rhodamine B.

Reactions were run aerobically with 10 μ M rhodamine B, 1 mM ascorbate, and 1 μ M M-chelate, with and without 1 mM H₂O₂ in 20 mM Na₂HPO₄, pH 7.4, in a clear 96-well plate. The disappearance of rhodamine B was monitored via UV/vis at 555 nm on a Molecular Devices SPECTRA MAX M2 plate reader spectrophotometer. The overall change in absorbance, which corresponded to complete reaction of 10 μ M RhB, was used to convert units of absorbance into units of μ M RhB, and the initial rates (μ M RhB/min) were determined from initial slopes of the kinetic plots of absorbance over time.

Ascorbic Acid Consumption. Reactions were run aerobically with 10 μ M M-chelate and 1 mM ascorbic acid, with and without 1 mM H₂O₂, in 20 mM HEPES, 100 mM NaCl, pH 7.4, on a clear 96-well plate. The disappearance of reduced ascorbic acid was monitored via UV/vis at 300 nm on a Molecular Devices SPECTRA MAX M2 plate reader spectrophotometer. The overall change in absorbance, which corresponded to the complete reaction of 1 mM ascorbate, was used to convert units of absorbance into units of μ M ascorbate, and the initial rates (μ M ascorbate/min) were determined from initial slopes of the kinetic plots of absorbance over time.

Square Wave Voltammetry. Solutions of 1 mM M-chelates were formed in 20 mM HEPES, 100 mM NaCl, pH 7.4, under anaerobic conditions at ambient temperature. M-chelate ratios used ranged from 1:1.5 to 1:2, but were adjusted to 1:1.2 for TACN to minimize the possibility of M-(TACN)₂ complex formation. For each experiment, buffers, reagents, and the electrochemical cell were vacuum- and argon-purged before complex formation. Reduction potentials for each metal complex were determined via square wave voltammetry using an EG&G Princeton Applied Research potentiostat/galvanostat with glassy carbon working electrode, Ag/AgCl reference electrode, and platinum auxiliary electrode, and the potential was determined by fitting to Gaussian eq 6. *Y* and *V* are the measured variable current and variable applied potential, respectively; *Y*₀ and *V*_C are the fitted baseline current and fitted reduction potential, respectively; *A*, *w*, and *m* are the fitted peak area, peak width, and baseline current slope, respectively. Instrument parameters were established with Int. = 10 mV, Freq. = 100 Hz, *I* = 10⁻⁴ A. Potentials vs Ag/AgCl were converted to potentials vs NHE.

$$Y = A/[w(\pi/2)^{1/2}] \exp[-2\{(V - V_C)^2/w^2\}] + mV + Y_0 \quad (6)$$

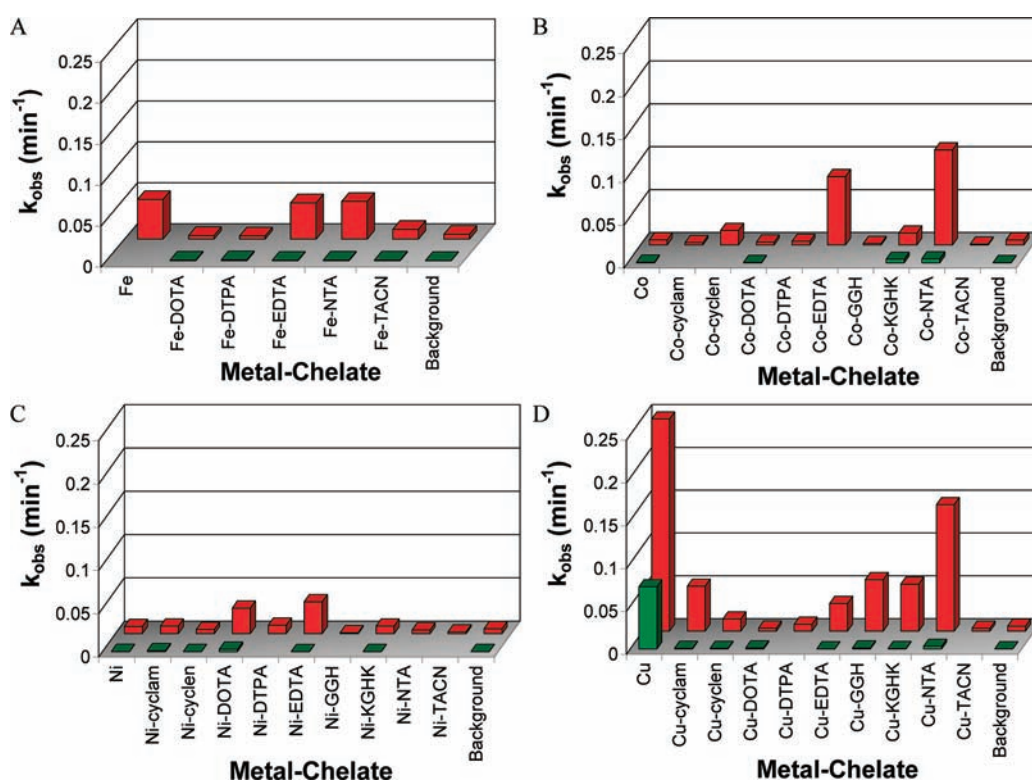


Figure 1. Summary of observed first-order rate constants (k_{obs}) for consecutive DNA nicking (k_{nick} , rear) and subsequent linearization (k_{lin} , front) by each M-chelate: (A) Fe complexes, (B) Co complexes, (C) Ni complexes, and (D) Cu complexes.

RESULTS

DNA Cleavage. Rate constants for nicking and linearization of plasmid DNA by each metal-chelate in the presence of 1 mM H_2O_2 and 1 mM ascorbate are summarized in Figure 1. These were obtained by fitting gel electrophoresis product intensities to a first-order consecutive reaction model (defined by eqs 1–3), as shown in Figure 2. Plasmid nicking rates above the limit of detection (Table 1) were observed for the following complexes in order of decreasing rate: $\text{Cu}^{2+}(\text{aq}) > \text{Cu-NTA} > \text{Co-NTA} > \text{Co-EDTA} > \text{Cu-GGH} > \text{Cu-KGHK} > \text{Cu-cyclam} > \text{Fe}^{2+}(\text{aq}) > \text{Fe-NTA} > \text{Fe-EDTA} > \text{Ni-EDTA} > \text{Cu-EDTA} > \text{Ni-DOTA} > \text{Co-cyclen} > \text{Co-KGHK} > \text{Cu-cyclen} > \text{Fe-TACN}$. Among metals, copper complexes generally demonstrated the highest reactivity, while NTA complexes showed the highest reactivity among chelators.

Ascorbate Consumption. Ascorbate consumption experiments were used to measure the relative rate with which each oxidized M-chelate could be re-reduced in a multiple-turnover redox cycle. The 300 nm absorbance of 1 mM ascorbate was monitored over time in reactions with each M-chelate under aerobic conditions, both with and without 1 mM H_2O_2 . The concentration of ascorbate in each assay was initially 100-fold higher than the M-chelate concentration (10 μM), and ascorbate consumption was therefore used as a measure of the number of turnovers promoted by M-chelate reactivity. Initial rates of ascorbate consumption resulting from $\text{H}_2\text{O}_2/\text{M-chelate}$ or $\text{O}_2/\text{M-chelate}$ were distinguished by subtraction (data obtained with H_2O_2 as a co-reactant, minus data obtained in the absence of H_2O_2), and the resulting data points are summarized in Figure 3 and Table 1. Initial rates of ascorbate consumption resulting from $\text{H}_2\text{O}_2/\text{M-chelate}$ reactivity that were greater than the limit of

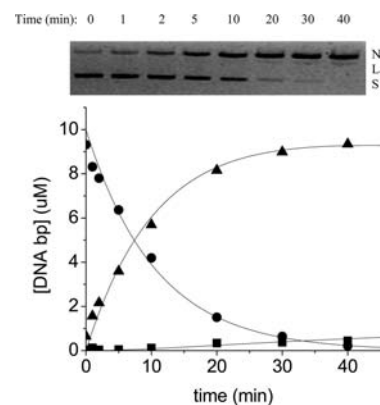


Figure 2. Time-dependent cleavage of plasmid DNA by Cu-NTA. (Top) Conversion of plasmid DNA from supercoiled (S) to nicked (N) to linear (L) form, monitored by agarose gel electrophoresis. (Bottom) Variation of the relative concentrations of supercoiled, nicked, and linear form DNA and fitting to a first-order consecutive reaction model (S = ●; N = ▲; L = ■).

detection were observed for the following complexes in order of decreasing rate: $\text{Fe-NTA} > \text{Fe-EDTA} > \text{Cu}^{2+}(\text{aq}) > \text{Fe-TACN} > \text{Fe}^{2+}(\text{aq}) > \text{Cu-GGH}$. Similarly, initial rates resulting from $\text{O}_2/\text{M-chelate}$ reactivity above the limit of detection were observed for the following complexes in order of decreasing rate: $\text{Cu}^{2+}(\text{aq}) > \text{Co-KGHK} > \text{Fe-EDTA} > \text{Fe-TACN} > \text{Co-GGH} > \text{Fe-NTA} > \text{Cu-NTA}$. Only $\text{Cu}^{2+}(\text{aq})$, Fe-EDTA, Fe-NTA, and Fe-TACN were observed to consume ascorbate with either O_2 or H_2O_2 as co-reactant. Other complexes, Co-GGH, Co-KGHK, and Cu-NTA, were observed to consume ascorbate only with O_2 as

Table 1. Summary of Observed Rate Constants for DNA Nicking Reactions (k_{nick}) Promoted by M-Chelates/ H_2O_2 /Ascorbate^a

complex	k_{nick} for DNA nicking (min^{-1})	ascorbate consumption rate for H_2O_2 and $\{\text{O}_2\}$ ($\mu\text{M}/\text{min}$)	TEMPO reaction rate for H_2O_2 and $\{\text{O}_2\}$ ($\mu\text{M}/\text{min}$)	reduction potential vs NHE (mV)
Fe	0.05 ± 0.01	$6.4 \pm 0.1 \{-^b\}$	$-^b \{-^b\}$	$-^c$
Fe-DOTA	$-^b$	$-^b \{-^b\}$	$0.0601 \pm 0.0005 \{-^b\}$	396^{39}
Fe-DTPA	$-^b$	$-^b \{-^b\}$	$0.0185 \pm 0.0005 \{-^b\}$	280^{39}
Fe-EDTA	0.044 ± 0.009	$80 \pm 10 \{6.9 \pm 0.2\}$	$0.078 \pm 0.001 \{0.0222 \pm 0.0006\}$	391^{39}
Fe-NTA	0.05 ± 0.01	$130 \pm 20 \{4.15 \pm 0.04\}$	$0.145 \pm 0.002 \{0.0449 \pm 0.0005\}$	464^{39}
Fe-TACN	0.012 ± 0.006	$17 \pm 1 \{5.7 \pm 0.1\}$	$25.94 \pm 0.02 \{0.0099 \pm 0.0001\}$	175^d
Co	$-^b$	$-^b \{-^b\}$	$0.0319 \pm 0.0009 \{-^b\}$	$-^c$
Co-Cyclam	$-^b$	$-^b \{-^b\}$	$0.0175 \pm 0.0002 \{-^b\}$	61^d
Co-Cyclen	0.017 ± 0.003	$-^b \{-^b\}$	$-^b \{0.0124 \pm 0.0002\}$	-228^d
Co-DOTA	$-^b$	$-^b \{-^b\}$	$-^b \{-^b\}$	142^{39}
Co-DTPA	$-^b$	$-^b \{-^b\}$	$-^b \{-^b\}$	1111^{39}
Co-EDTA	0.08 ± 0.02	$-^b \{-^b\}$	$0.0185 \pm 0.0003 \{-^b\}$	146^{39}
Co-GGH	$-^b$	$0.5 \pm 0.2 \{4.9 \pm 0.1\}$	$-^b \{-^b\}$	-119^{39}
Co-KGHK	0.014 ± 0.002	$0.5 \pm 0.2 \{7.1 \pm 0.2\}$	$-^b \{-^b\}$	-228^{39}
Co-NTA	0.1 ± 0.1	$-^b \{-^b\}$	$0.075 \pm 0.002 \{-^b\}$	274^{39}
Co-TACN	$-^b$	$-^b \{-^b\}$	$-^b \{-^b\}$	-362^d
Ni	$-^b$	$-^b \{-^b\}$	$0.0156 \pm 0.0003 \{-^b\}$	$-^c$
Ni-Cyclam	$-^b$	$-^b \{-^b\}$	$-^b \{-^b\}$	-275^d
Ni-Cyclen	$-^b$	$-^b \{-^b\}$	$-^b \{-^b\}$	-211^d
Ni-DOTA	0.030 ± 0.007	$-^b \{-^b\}$	$-^b \{-^b\}$	-35^{39}
Ni-DTPA	$-^b$	$-^b \{-^b\}$	$-^b \{-^b\}$	$-^c$
Ni-EDTA	0.037 ± 0.002	$-^b \{-^b\}$	$-^b \{-^b\}$	172^{39}
Ni-GGH	$-^b$	$-^b \{-^b\}$	$-^b \{-^b\}$	1000^{39}
Ni-KGHK	$-^b$	$-^b \{-^b\}$	$-^b \{-^b\}$	1055^{39}
Ni-NTA	$-^b$	$-^b \{-^b\}$	$-^b \{-^b\}$	176^{39}
Ni-TACN	$-^b$	$-^b \{-^b\}$	$-^b \{-^b\}$	991^d
Cu	0.25 ± 0.05	$80 \pm 10 \{12.9 \pm 0.2\}$	$0.16 \pm 0.01 \{-^b\}$	136
Cu-Cyclam	0.053 ± 0.004	$-^b \{-^b\}$	$-^b \{-^b\}$	163^d
Cu-Cyclen	0.014 ± 0.004	$-^b \{-^b\}$	$-^b \{-^b\}$	280^d
Cu-DOTA	$-^b$	$-^b \{-^b\}$	$-^b \{-^b\}$	180^{39}
Cu-DTPA	$-^b$	$-^b \{-^b\}$	$-^b \{-^b\}$	148^{39}
Cu-EDTA	0.032 ± 0.003	$-^b \{-^b\}$	$-^b \{-^b\}$	47^{39}
Cu-GGH	0.06 ± 0.01	$2.72 \pm 0.08 \{-^b\}$	$-^b \{-^b\}$	1038^{39}
Cu-KGHK	0.055 ± 0.008	$-^b \{-^b\}$	$-^b \{-^b\}$	1058^{39}
Cu-NTA	0.148 ± 0.007	$0.72 \pm 0.05 \{3.46 \pm 0.04\}$	$-^b \{-^b\}$	215^{39}
Cu-TACN	$-^b$	$-^b \{-^b\}$	$-^b \{-^b\}$	110^d
background	0.006 ± 0.001	$0.6 \pm 0.6 \{0.3 \pm 0.1\}$	$0.007 \pm 0.003 \{0.0039 \pm 0.0007\}$	

^a Initial rates for ascorbate consumption (with and without H_2O_2 as an added co-reactant) and radical generation (again, with and without added H_2O_2), as well as the reduction potential for each M-chelate, are listed for comparison. Redox couples are $3+/2+$ for Fe, Co, Ni-ATCUN, and Cu-ATCUN complexes and $2+/1+$ for all other Ni and Cu complexes. ^b Below detection limit. ^c Not determined. ^d This work.

co-reactant, whereas $\text{Fe}^{2+}(\text{aq})$ and Cu-GGH were observed to consume ascorbate only with H_2O_2 as co-reactant. This analysis provided a practical measure of the relative selectivity of M-chelate complexes for H_2O_2 and O_2 co-reactants under experimental conditions that were similar to those used for DNA cleavage experiments. For those complexes that were observed to consume ascorbate in the absence of added H_2O_2 , additional tests conducted under varying levels of anaerobicity confirmed O_2 as a necessary co-reactant (Figure S1). The numbers of ascorbate turnovers promoted by each M-chelate after 6 h of incubation are listed in Table 2 (with and without added H_2O_2). The number of turnovers was generally higher in the presence of

H_2O_2 , although a few complexes, including Fe-EDTA, Fe-NTA, Fe-TACN, Co-GGH, Co-KGHK, $\text{Cu}^{2+}(\text{aq})$, and Cu-NTA, demonstrated similar turnover activity even in the absence of H_2O_2 , consistent with the observed initial rates of ascorbate consumption reflecting reaction with O_2 . Ascorbate turnovers above background reactivity were observed for 21 of the 36 complexes tested in the presence of H_2O_2 .

Radical Generation. The fluorescent molecule TEMPO-9-AC contains a nitroxide radical that results in internal quenching of fluorescence.^{40,41} Following reaction with either hydroxyl or superoxide radicals, the nitroxide radical is converted to a non-radical species (Supporting Information, Figure SM7), and the

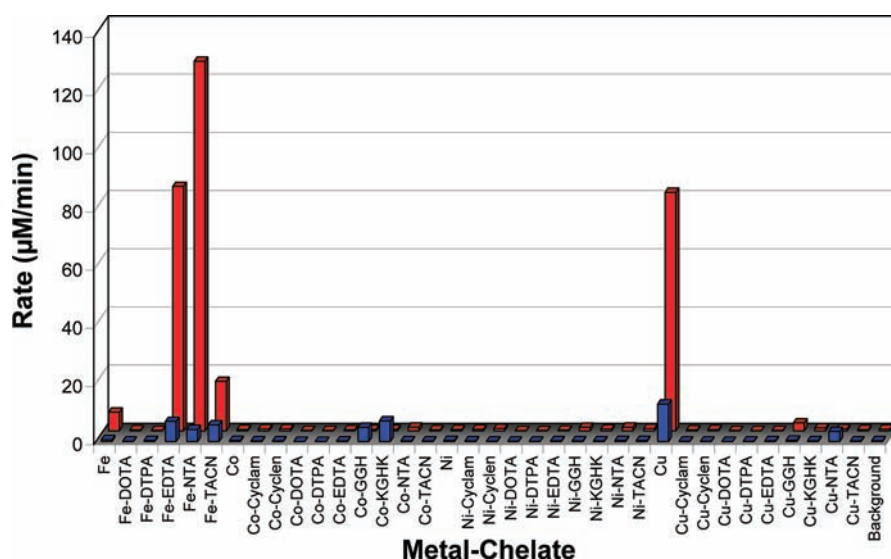


Figure 3. Summary of initial rates for multiple-turnover consumption of ascorbate by each M-chelate/ O_2 (front) and M-chelate/ H_2O_2 (rear) combination.

fluorescence is restored.^{42–44} To investigate the relative rate of diffusible radical production by each M-chelate with each of the co-reactants H_2O_2 or O_2 , each M-chelate was reacted with the TEMPO-9-AC radical (1:1 stoichiometry) under aerobic conditions with and without added 1 mM H_2O_2 and monitored by real-time fluorimetry. The steady-state rates of TEMPO conversion were thereby determined and provided a quantitative measure of diffusible radical production. As with the ascorbate consumption results, steady-state rates of TEMPO conversion resulting from H_2O_2 /M-chelate or O_2 /M-chelate reactions were distinguished by subtraction (data obtained with H_2O_2 as a co-reactant, minus data obtained in the absence of H_2O_2), and the resulting data points are summarized in Figure 4 and Table 1. Rates of TEMPO conversion resulting from H_2O_2 /M-chelate activity that were greater than the limit of detection were observed for the following complexes in order of decreasing rate: Fe-TACN \gg $Cu^{2+}(aq)$ > Fe-NTA > Fe-EDTA > Co-NTA > Fe-DOTA > $Co^{2+}(aq)$ > Fe-DTPA \sim Co-EDTA > Co-cyclam > $Ni^{2+}(aq)$. Similarly, initial rates resulting from O_2 /M-chelate reactivity above the limit of detection were observed for the following complexes in order of decreasing rate: Fe-NTA > Fe-EDTA > Co-cyclen > Fe-TACN. The complexes Fe-EDTA, Fe-NTA, and Fe-TACN were observed to produce radicals with either O_2 or H_2O_2 as co-reactant.

To differentiate between hydroxyl and superoxide radicals as reactive species, the reaction with rhodamine B (RhB), which reacts specifically with hydroxyl radicals (Supporting Information, Figure SM7),^{18,45,46} was also studied. The combination of RhB and TEMPO-9-AC reaction data allowed discrimination between hydroxyl and superoxide radicals produced by each M-chelate following reaction with 10 μ M RhB and 1 mM ascorbate, with and without 1 mM H_2O_2 . The decrease in RhB absorbance was attributed to reaction with hydroxyl radical. Rates of RhB reaction resulting from H_2O_2 /M-chelate or O_2 /M-chelate reactivity were determined by subtraction (Figure S5). Reactions resulting from H_2O_2 /M-chelate in the presence of ascorbate and determined to be above the limit of detection were observed for the following complexes in order of decreasing initial rate: Fe-NTA > Fe-EDTA > $Cu^{2+}(aq)$ \sim Cu-GGH. The rate observed for Cu-NTA was similar

to the limit of detection. Rates resulting from reaction of O_2 /M-chelate in the presence of ascorbate were found to be up to 100-fold slower, with the exception of $Cu^{2+}(aq)$, but determined to be above the limit of detection in the order $Cu^{2+}(aq)$ > Fe-EDTA > Fe-NTA.

Reduction Potentials. M-chelate reduction potentials were determined by square-wave voltammetry using solution conditions (pH 7.4) similar to those used in the DNA cleavage, ascorbate consumption, and TEMPO experiments, with the exception that these electrochemical experiments were conducted under anaerobic conditions. A summary of observed reduction potentials is listed in Table 1, and as expected, these were significantly modulated by the chelator. In general, M-chelates that were observed to cleave DNA under the reaction conditions employed demonstrated reduction potentials in the range -500 to 500 mV, with the exception of the Cu-ATCUN complexes (Cu-GGH and Cu-KGHK) with reduction potentials of 1038 and 1058 mV, respectively, reflecting the distinct Cu^{3+}/Cu^{2+} redox couple exhibited by these two species.

DMSO Inhibition of DNA Cleavage. Both TEMPO and rhodamine experiments supported reactivity through the action of either a free diffusible or metal-associated hydroxyl radical species. M-chelate complexes observed to cleave DNA were retested for DNA cleavage in the presence of variable concentrations of DMSO, a hydroxyl radical scavenger.^{18,22} These DMSO inhibition experiments were performed in order to distinguish reactivity from free diffusible radicals versus a metal-associated radical that was held in close proximity to the DNA by virtue of the metal complex. That is, to distinguish between two possible pathways, namely: (1) the extent to which diffusible radicals were the active intermediates in DNA cleavage, or (2) the extent to which radical-generating M-chelates were tightly associated to the DNA, since a DNA-bound M-chelate would require a shorter distance for radical migration before colliding with DNA.²² The IC_{50} values were measured (Figure 5), and the following active complexes were strongly inhibited by DMSO: Cu-cyclam, Co-cyclen, Co-NTA, Fe, Fe-NTA, Ni-EDTA, Fe-EDTA, Co-EDTA, Cu-cyclen, and Ni-DOTA. Complexes with little to no observable DMSO inhibition included $Cu^{2+}(aq)$, Cu-EDTA, Cu-GGH, Cu-KGHK, Co-KGHK, Cu-NTA, and Fe-TACN. The

Table 2. Number of Turnovers Observed for Ascorbate (μM Ascorbate Consumed/ μM M-Chelate), Promoted by Each M-Chelate in the Presence ($\text{H}_2\text{O}_2 + \text{O}_2$) and Absence (O_2 only) of H_2O_2

complex	obsd no. of ascorbate turnovers ^a	
	with H_2O_2	without H_2O_2
Fe	≥ 100	20 ± 10
Fe-DOTA	18 ± 2	5 ± 1
Fe-DTPA	≥ 100	13 ± 2
Fe-EDTA	≥ 100	≥ 100
Fe-NTA	≥ 100	≥ 100
Fe-TACN	≥ 100	≥ 100
Co	31 ± 3	20 ± 10
Co-cyclam	30 ± 3	8 ± 4
Co-cyclen	32 ± 4	8 ± 3
Co-DOTA	9 ± 2	4 ± 1
Co-DTPA	8 ± 2	4 ± 1
Co-EDTA	21 ± 4	8 ± 2
Co-GGH	≥ 100	≥ 100
Co-KGHK	≥ 100	≥ 100
Co-NTA	54 ± 5	9 ± 2
Co-TACN	21 ± 4	8 ± 2
Ni	29 ± 3	10 ± 10
Ni-cyclam	27 ± 3	10 ± 10
Ni-cyclen	33 ± 4	6 ± 4
Ni-DOTA	9 ± 2	6 ± 1
Ni-DTPA	8 ± 2	5 ± 1
Ni-EDTA	20 ± 4	11 ± 2
Ni-GGH	40 ± 10	9 ± 2
Ni-KGHK	30 ± 8	9 ± 2
Ni-NTA	57 ± 5	12 ± 2
Ni-TACN	40 ± 10	12 ± 2
Cu	≥ 100	≥ 100
Cu-cyclam	18 ± 3	6 ± 4
Cu-cyclen	21 ± 3	6 ± 4
Cu-DOTA	8 ± 2	4 ± 1
Cu-DTPA	8 ± 2	5 ± 1
Cu-EDTA	15 ± 4	11 ± 2
Cu-GGH	≥ 100	17 ± 2
Cu-KGHK	44 ± 7	11 ± 2
Cu-NTA	≥ 100	≥ 100
Cu-TACN	22 ± 4	8 ± 2
none ^b	20 ± 3	20 ± 10

^a The maximum possible number of turnovers that could be observed was 100, since the concentrations of ascorbate and metal complex used were $1000 \mu\text{M}$ and $10 \mu\text{M}$, respectively, and numbers for complexes that completely consumed $1000 \mu\text{M}$ ascorbate are listed as ≥ 100 . Above-background numbers are shown in bold. ^b Background values were calculated the same way as for M-chelates, although no M-chelate was present.

low level of background reactivity (no complex), which was likely the result of a very low concentration of solution radicals generated by the uncatalyzed reaction of H_2O_2 and ascorbate, was also strongly inhibited by DMSO.

DNA Residency Time. Relative rates of DNA linearization vs rates of DNA nicking were assessed, and a statistical ratio of the

probable number of double-strand DNA cuts (n_2) versus the probable number of single-strand DNA nicks (n_1) was established for each M-chelate following reaction with DNA. Complexes with $n_2/n_1 < 0.01$ promote DNA linearization by a random nicking pathway that results in linearization only when two random nicks on opposite strands of dsDNA occur sufficiently close together to result in linearization.^{18,38} Complexes with an n_2/n_1 ratio significantly greater than 0.01 promote linearization of DNA by a concerted mechanism, where a bound complex mediates nicking of both strands during its residency time and within the narrow locus of the binding site. This concerted pathway and subsequent fast linearization are more likely to occur for complexes that have a higher affinity for DNA and thus have a longer residency time when bound to the DNA. Among the complexes found to cleave DNA, the n_2/n_1 ratios were determined and are summarized in Figure 6. The degree to which nicking and linearization was concerted was found to decrease in the following order: $\text{Cu}^{2+}(\text{aq}) > \text{Co-KGHK} > \text{Ni-DOTA} > \text{Fe-NTA} \sim \text{Fe-TACN} \sim \text{Fe-EDTA} > \text{Cu-KGHK} > \text{Cu-NTA} > \text{Cu-GGH} \sim \text{Ni-EDTA} \sim \text{Cu-EDTA} > \text{Fe}^{2+}(\text{aq}) \sim \text{Cu-cyclam} \sim \text{Cu-cyclen} \sim \text{Co-cyclen} \sim \text{Co-EDTA} \sim \text{Co-NTA}$. Since a highly concerted DNA linearization reaction requires a fast linearization step following the initial nicking reaction, a correlation between the n_2/n_1 ratio and the ratio of the rate constants of consecutive nicking and linearization ($k_{\text{lin}}/k_{\text{nick}}$) was expected. Indeed, such a correlation was observed (Figure 7).

DISCUSSION

DNA Cleavage and Reduction Potential. DNA cleavage by the M-chelates described herein was mediated by the generation of reactive oxygen species (ROS). The ability of M-chelates to generate reactive intermediates is directly related to their ability to switch between oxidation states and promote formation of ROS through redox chemistry with biological co-reactants such as H_2O_2 , O_2 , and ascorbate. Given that reported reduction potentials at neutral pH for $\text{O}_2/\text{superoxide}$, $\text{superoxide}/\text{H}_2\text{O}_2$, $\text{H}_2\text{O}_2/\text{HO}^\bullet$, and ascorbyl radical/ascorbate are -330 , 890 , 380 , and -66 mV, respectively,^{47,48} single-electron oxidation/reduction by $\text{H}_2\text{O}_2/\text{ascorbate}$ is thermodynamically favored for M-chelates with reduction potentials in the range from 380 to -66 mV. Indeed, the most reactive M-chelates displayed reduction potentials within this range (Table 1 and Figure 8), further suggesting that the most rapid rates of DNA cleavage reflected multiple-turnover generation of hydroxyl radicals. We have recently observed a similar trend for targeted cleavage of HIV-1 Rev Response Element RNA by Rev-coupled M-chelates.³⁹ M-chelate-mediated reduction of dioxygen is also possible, although direct superoxide generation is less thermodynamically favored ($E^\circ = -330$ mV). A few M-chelates with reduction potentials exceeding 1000 mV also demonstrated modest levels of DNA cleavage activity (Cu-GGH and Cu-KGHK), though the more moderate activity levels most likely reflect the extent to which these complexes lie outside of the optimum potential range. The reduction potentials for these ATCUN complexes are such that the oxidation of substrate is strongly thermodynamically favored but the prerequisite generation of the oxidized metal is not favored, and so these two complexes show relatively low reactivity. The relative sluggishness of the metal-ATCUN-promoted redox chemistry is most likely important for the natural physiological roles of these motifs, where the slower cellular release of ROS would be advantageous.^{19,20,31,49–53}

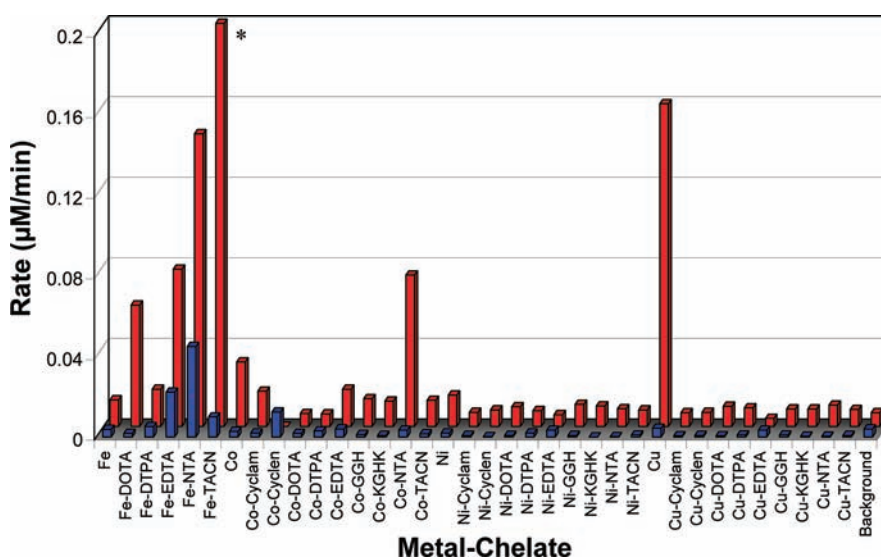


Figure 4. Summary of steady-state rates of TEMPO-9-AC-monitored radical generation for each M-chelate/O₂ (front) and M-chelate/H₂O₂ (rear) combination. *Fe-TACN/H₂O₂ was observed to promote very rapid reaction relative to other catalysts, requiring stopped-flow measurements to determine an observed rate of $25.94 \pm 0.02 \mu\text{M}/\text{min}$ with the conditions used.

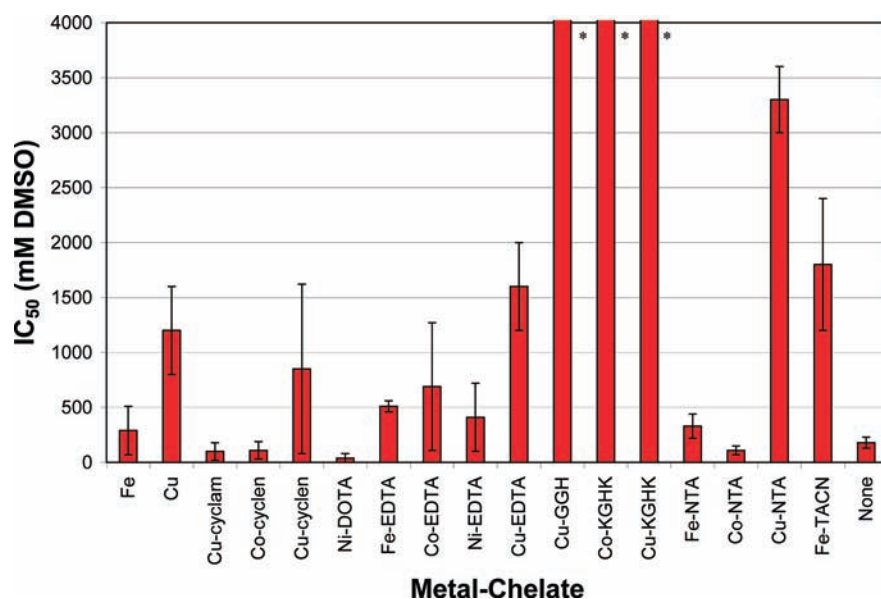


Figure 5. Summary of DMSO IC₅₀ inhibition values for DNA cleavage by M-chelates/H₂O₂/ascorbate. *IC₅₀ >> 1000 mM.

DNA Cleavage and Ascorbate Consumption. The driving force behind the observed DNA cleavage chemistry ultimately stems from the oxidants (H₂O₂ or O₂) and the ascorbic acid reductant, while the critical catalytic role is performed by those M-chelates that catalyze the reaction between these co-reactants to form metal-associated ROS, which then react with and cleave the DNA.³⁰ In every case it was expected that the oxidant would first oxidize the M-chelate, forming an intermediate ROS with subsequent reduction of the M-chelate by ascorbate, allowing for multiple-turnover cycles of oxidation and reduction.⁵⁴ Indeed, with the exception of Co-GGH, every M-chelate species observed to consume ascorbate with multiple turnovers was also found to cleave DNA under the conditions used (Table 1), although there was no clear quantitative correlation between the

rate of DNA cleavage and the rate of ascorbate consumption. A few M-chelate complexes were observed to cleave DNA but did not undergo multiple-turnover consumption of ascorbate. These complexes (Cu-cyclam, Co-cyclen, Cu-cyclen, Ni-DOTA, Co-EDTA, Ni-EDTA, Cu-EDTA, Cu-KGHK, Co-NTA) most likely operate either by a single-turnover oxidative mechanism, by a multiple-turnover mechanism in which DNA is directly oxidized by the M-chelate and reduction by ascorbate was unnecessary for regeneration of the reduced M-chelate, or by a hydrolytic mechanism. Consistent with these observations, Co(III)-cyclen complexes are known to hydrolyze DNA at a slow rate ($k_{\text{obs}} \approx 0.0003 \text{ min}^{-1}$ with 1 mM complex),^{55,56} although an oxidative mechanism is also possible for [Co-cyclen]^{2+/3+} with co-reactants. An alternative explanation for a reduction in, or the absence of,

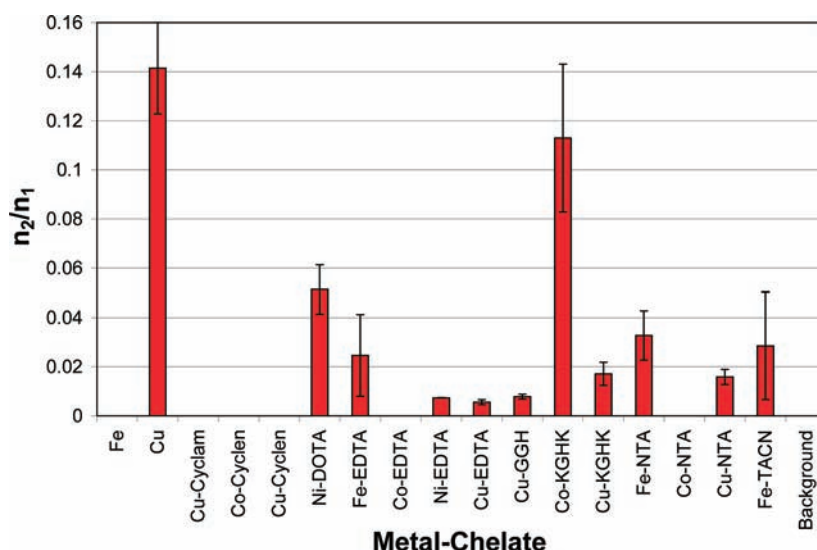


Figure 6. Summary of n_2/n_1 ratios resulting from a Freifelder–Trumbo analysis of DNA cleavage reactivity by M-chelates. M-chelates with $n_2/n_1 = 0$ had no quantifiable linearized DNA.

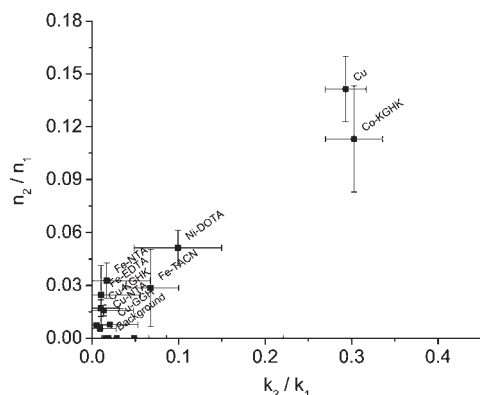


Figure 7. Correlation between the ratio of double and single strand breaks (n_2/n_1) and the ratio of rate constants for linearization and nicking (k_{lin}/k_{nick}).

multiple turnovers in ascorbate consumption is that the M-chelate catalysts are inactivated as a result of oxidation by the ROS formed, with M-chelates that show a higher number of turnovers being less susceptible to inactivation under the conditions used.

DNA Cleavage and Radical Generation. M-chelates known to generate diffusible hydroxyl radicals in combination with H_2O_2 (Fe-EDTA, Fe-NTA, Cu-GGH, and $Cu^{2+}(aq)$) provide significant DNA cleavage when combined with H_2O_2 /ascorbate. They also prompt a strong response in both the TEMPO radical assay and rhodamine B consumption assays, consistent with hydroxyl radicals promoting the observed DNA cleavage by these M-chelates. However, aside from these complexes, there was very little correlation between diffusible radical generation and DNA cleavage rate, suggesting that diffusible radicals were not very efficient at mediating DNA cleavage. For example, Fe-DTPA, Fe-DOTA, Co-cyclam, $Ni^{2+}(aq)$, and $Co^{2+}(aq)$ were each observed to readily generate radicals as monitored by TEMPO-9-AC, but none of these compounds were observed to cleave DNA under similar reaction conditions. Conversely, $Fe^{2+}(aq)$, Cu-cyclam, Cu-cyclen, Ni-DOTA, Cu-EDTA, Ni-EDTA,

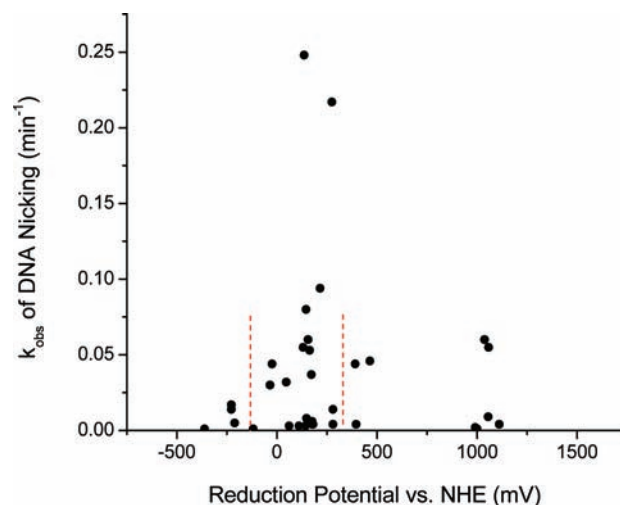


Figure 8. Rate constants for DNA nicking by M-chelates were observed to be highest for M-chelate complexes with reduction potentials between those of co-reactants ascorbate (-66 mV) and H_2O_2 (380 mV), indicated by the dashed lines.

Cu-KGHH, and Cu-NTA were observed to cleave DNA but were not observed to generate radical species in standard detection assays. In order for diffusible hydroxyl radicals produced by M-chelates to effect DNA cleavage when the M-chelate is used at 100 nM concentration, it appears to be necessary for the M-chelate to possess at least minimal binding interaction with the DNA, such that the origin of each hydroxyl radical was closer to the DNA than would occur in the absence of this type of interaction. Indeed, DNA cleavage by Cu-GGH, $Cu^{2+}(aq)$, and Fe-TACN was weakly inhibited by DMSO, relative to DNA cleavage by the low background concentration of solution radicals, in spite of the ability of DMSO to scavenge hydroxyl radicals. This is supported by a Freifelder–Trumbo analysis for DNA linearization by Fe-TACN, Fe-NTA, Fe-EDTA, and $Cu^{2+}(aq)$ that is consistent with the existence of unique binding interactions between these complexes and DNA (Table 3). The complexes Co-cyclen,

Table 3. DMSO Inhibition and Freifelder–Trumbo Analysis of DNA Cleavage by M-Chelates That Exhibited Cleavage Rates above the Limit of Detection (See Table 1)^a

complex	IC ₅₀ (mM DMSO)	<i>n</i> ₂ / <i>n</i> ₁
Cu	1200 ± 400	0.14 ± 0.01
Fe	300 ± 200	~0
Cu-cyclam	100 ± 80	~0
Cu-cyclen	900 ± 800	~0
Co-cyclen	110 ± 80	~0
Ni-DOTA	40 ± 40	0.05 ± 0.01
Cu-EDTA	1600 ± 400	0.01 ± 0.01
Ni-EDTA	400 ± 300	0.0073 ± 0.0001
Co-EDTA	700 ± 600	~0
Fe-EDTA	510 ± 50	0.03 ± 0.02
Cu-GGH	≫1000	0.01 ± 0.01
Cu-KGHK	≫1000	0.017 ± 0.005
Co-KGHK	≫1000	0.11 ± 0.03
Cu-NTA	3300 ± 300	0.016 ± 0.003
Co-NTA	110 ± 40	~0
Fe-NTA	300 ± 100	0.03 ± 0.01
Fe-TACN	1800 ± 600	0.03 ± 0.02
background	180 ± 50	~0

^a A low IC₅₀ is correlated to DNA nicking via diffusible radicals and/or weak binding of the M-chelate to DNA. Those M-chelates displaying a ratio of *n*₂/*n*₁ > 0.01 linearize the DNA via a concerted mechanism as a result of the higher residency time (tighter binding) for the DNA complex.

Co-EDTA, and Co-NTA promoted significant DNA cleavage and a moderate response to the TEMPO-9-AC radical assay but did not provide a response in the rhodamine B assay, making the assignment of hydroxyl radicals as the active species more problematic. However, Co-cyclen, Co-NTA, and Co-EDTA were each strongly inhibited by DMSO, and a Freifelder–Trumbo analysis of DNA linearization/nicking by Co-cyclen, Co-NTA, and Co-EDTA indicated no association between these complexes and DNA (Table 3), suggesting that DNA cleavage by these complexes was indeed mediated by diffusible radicals. Together these data support the hypothesis that radical-mediated DNA cleavage is most efficient for M-chelates that possess binding interactions with the DNA. Among these complexes, the data also suggest that DNA cleavage by diffusible radicals is inherently less efficient than by metal-bound ROS, consistent with the expectation that metal-bound reactive oxygen intermediates would more efficiently cleave the DNA as a result of their prolonged proximity to the DNA.

Ascorbate Consumption, Radical Generation, and Reduction Potential. As expected, multiple turnover rates for ascorbate consumption and radical generation by M-chelates were found to be dependent on M-chelate reduction potentials (Figure 9). A similar trend was observed for DNA cleavage rates (Figure 8). Ascorbate consumption by M-chelates and the co-reactant H₂O₂ was also observed to be fastest for those complexes with reduction potentials in the range of –66 to +380 mV (Figure 9), which correspond to the reduction potentials of ascorbyl radical/ascorbate and H₂O₂/HO[•], respectively. As observed for native superoxide dismutase enzymes, which possess reduction potentials similarly poised between those of the relevant half-reaction redox pairs (O₂/superoxide and superoxide/H₂O₂),^{57,58} reduction potentials for M-chelates between –66 and +380 mV would result in an overall favorable thermodynamic

profile for oxidation by H₂O₂ and reduction by ascorbate, thereby promoting multiple oxidation/reduction cycles. When radical generation by M-chelate/H₂O₂ conditions was monitored by the TEMPO-9-AC reaction, turnover was observed to be fastest for complexes with reduction potentials less than +380 mV, such that conversion of H₂O₂ to hydroxyl radical was thermodynamically favored (Figure 9). Therefore, the most likely mechanism for reaction of M-chelate/H₂O₂/ascorbate involves Fenton-style single-electron reduction of H₂O₂ to form hydroxyl radicals, followed by reduction of the oxidized metal by ascorbate. The hydroxyl radicals produced by these reactions could be either diffusible or metal-bound. In that regard, the M-chelate/H₂O₂ reactions that generated radicals as monitored by TEMPO-9-AC most likely contain those M-chelates that produce diffusible hydroxyl radicals. Hydroxyl radical generation by Cu²⁺(aq)/O₂ was ascorbate-dependent, as evidenced by comparison of TEMPO and RhB data.

The rate of ascorbate consumption by M-chelates in the presence of the co-reactant O₂ provided a similar, although slightly broader dependence on reduction potentials, and the data support reaction pathways involving either the thermodynamically unfavorable single-electron reduction of O₂ (*E*^o_{O₂/superoxide} = –330 mV) or the favorable two-electron reduction of O₂ (*E*^o_{O₂/H₂O₂} = 560 mV). Of the seven M-chelates that demonstrated significant rates of ascorbate consumption driven by O₂, only Fe-EDTA, Fe-NTA, and Fe-TACN were also observed to generate radicals under similar conditions in the absence of ascorbate (that is, TEMPO experiments conducted aerobically with no added ascorbate). Therefore, in the presence of both O₂ and ascorbate, reactions of Fe-EDTA, Fe-NTA, and Fe-TACN most likely proceeded via single-electron reduction of oxygen to form superoxide radical, with regeneration of reduced M-chelate by ascorbate. By contrast, other M-chelates (Co-GGH, Co-KGHK, Cu-NTA, Cu²⁺(aq)) that also show significant rates of O₂-driven ascorbate consumption but do not generate radicals under similar reaction conditions in the absence of ascorbate (TEMPO experiments with O₂ only) proceed either by two-electron reduction of O₂ to the peroxy state or by single-electron reduction of O₂ to form non-diffusible metal-bound superoxide. With the exception of Cu²⁺(aq), both pathways show consistency through the absence of detectable diffusible radicals with the O₂/M-chelate/ascorbate combination. Interestingly, radical generation by the O₂/Cu²⁺(aq) combination required the presence of ascorbate (radicals observed in the RhB/O₂/ascorbate assay but not in the TEMPO/O₂ assay), and the observed radicals were most likely hydroxyl radicals (supported by the RhB assay), suggesting the stepwise three-electron reduction of O₂ to hydroxyl radical for Cu²⁺(aq), in which release of the superoxide radical and peroxide intermediates did not occur to an appreciable extent.

Ascorbate consumption by M-chelates/O₂ was generally found to be slower than observed for M-chelates in the presence of H₂O₂, with the exceptions of Co-GGH, Co-KGHK, and Cu-NTA, suggesting that under the conditions used the reaction with O₂ was faster than with H₂O₂ for only these three complexes. Cobalt-ATCUN complexes such as Co-GGH and Co-KGHK show relatively low reduction potentials, –119 and –228 mV, respectively, and the thermodynamically unfavorable reduction of these complexes would become favorable if coupled with two-electron reduction of O₂ to H₂O₂ (*E*^o_{O₂/H₂O₂} = 560 mV). Alternatively, it is possible that the instability of the reduced Co-GGH and Co-KGHK species actually increased their

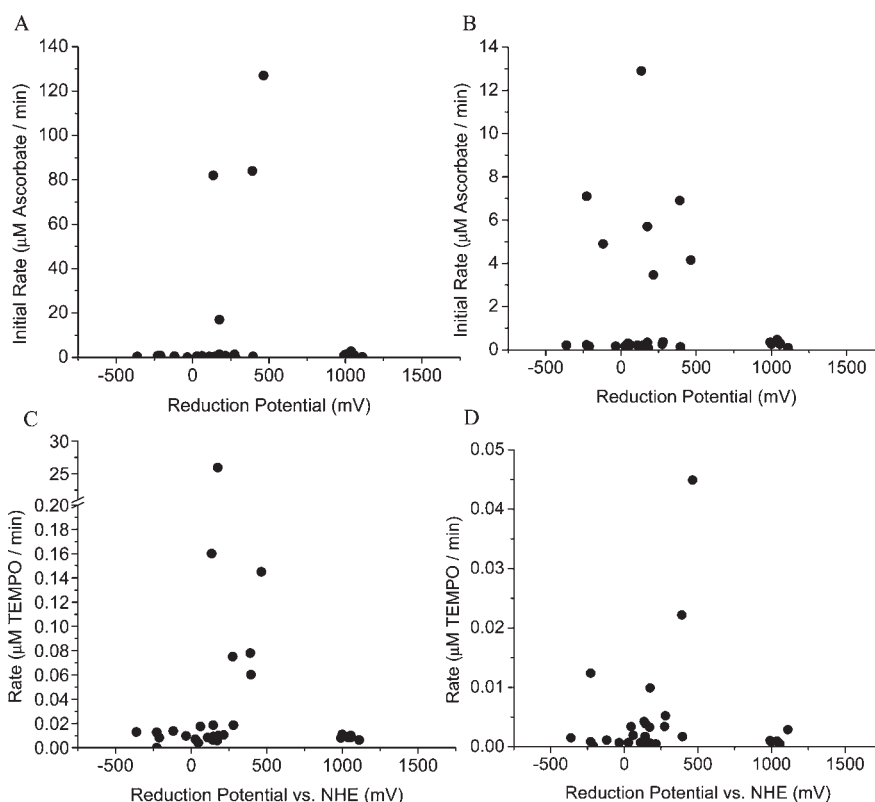


Figure 9. The highest rates of multiple-turnover ascorbate consumption and radical generation were found for M-chelates with biologically relevant reduction potentials. (A) Ascorbate consumption by M-chelate/ H_2O_2 . (B) Ascorbate consumption by M-chelate/ O_2 . (C) Radical generation by M-chelate/ H_2O_2 . (D) Radical generation by M-chelate/ O_2 .

reactivity with O_2 , facilitating the otherwise unfavorable formation of non-diffusible superoxide ($E^\circ_{\text{O}_2/\text{superoxide}} = -330 \text{ mV}$).

Effect of DNA-Binding Affinity on DNA Cleavage. It is expected that DNA cleavage rates are favorably influenced in the case of M-chelates that bind DNA with higher affinity, since ROS produced by M-chelates with higher DNA-binding affinity are on average closer to the DNA and thus are more likely to react with DNA within a given time frame. DNA-binding affinity is generally governed by one or more factors that include electrostatic attraction to the phosphate backbone, intercalation, and/or H-bonding. The variety of expected binding modes of the M-chelates, and the modest to weak levels of binding expected, make the use of fluorescent intercalator displacement (FID) assays inappropriate for the comparison of DNA-binding affinities. Negatively charged M-chelates, such as those formed by use of the ligands EDTA, DTPA, and DOTA, are typically thought to possess very low DNA-binding affinity due to repulsion of the negatively charged phosphate backbone of DNA, and DNA cleavage reactions mediated by those M-chelates are most likely mediated by diffusible radicals. In fact, the choice of EDTA for typical iron-mediated hydroxyl radical footprinting experiments reflects the poor binding of DNA by $[\text{Fe-EDTA}]^{-2-}$.⁵⁹ Positively charged M-chelates, such as those formed with ligands cyclam, cyclen, and TACN (and free metal ions), have been shown to display higher affinity toward DNA as a result of attraction toward the negatively charged backbone of DNA.²² Free $\text{Cu}^{2+}(\text{aq})$ has been shown to bind dsDNA non-specifically with a dissociation constant of $42 \mu\text{M}$, although in a few cases cooperative copper binding sites for dsDNA have been identified with significantly higher affinity.⁶⁰ Troglor and

co-workers have shown the complex $[\text{Fe-TACN}]^{3+/2+}$ to exhibit higher DNA-binding affinity than $[\text{Fe-EDTA}]^{-2-}$,²² consistent with the results of this study. A consistent though modest charge affect has also been documented by Huang and co-workers in the case of the tripeptide complexes $[\text{Ni-GGH}]^-$ and $[\text{Ni-KGH}]^+$, with dissociation constants for DNA binding of 26 and 14 nM, respectively.⁶¹ Prior studies from our laboratory have demonstrated modestly faster DNA cleavage by micromolar levels of Cu-KGHK relative to Cu-GGH;¹⁸ however, at the lower concentration used in this work (100 nM rather than $>4 \mu\text{M}$), the copper complexes of GGH and KGHK showed comparable low levels of activity. Positively charged metal complexes of cyclam, cyclen, and TACN demonstrated moderate rates of DNA cleavage. However, several negatively charged metal complexes with NTA and EDTA show markedly higher rates of DNA cleavage. In summary, the highly variable DNA cleavage rates and mechanisms observed for the M-chelates used in this study highlight the fact that, while DNA-binding affinity may somewhat skew the DNA cleavage rates, neither DNA binding nor redox activity is solely responsible for the observed nuclease activity. Rather, it is likely that specific combinations of DNA-binding affinity, DNA alignment, and redox mechanisms are more effective than others.

Predicted Mechanisms of Observed DNA Cleavage. Mechanisms of observed DNA cleavage by M-chelates were predicted for each M-chelate on the basis of the co-reactant dependence of ascorbate consumption and radical generation, the extent of DMSO inhibition of DNA cleavage, and the extent to which DNA nicking and linearization were concerted (Freifelder–Trumbo analysis). DNA cleavage by $\text{Cu}^{2+}(\text{aq})$

Table 4. Comparison of Second-Order Rate Constants for DNA Nicking Promoted by Several M-Chelate Complexes and DNA Cleavage by Other Artificial Nucleases

complex	substrate	$k_{2,\text{nick}}$ ($\text{M}^{-1} \text{min}^{-1}$)	co-reagent(s)	conditions	ref/note
$[\text{Cu-NTA}]^{-2-}$	dsDNA	1 420 000	ascorbate + H_2O_2	pH 7.4, 37 °C	<i>a</i>
$[\text{Co-NTA}]^{0-}$	dsDNA	900 000	ascorbate + H_2O_2	pH 7.4, 37 °C	<i>a</i>
$[\text{Cu-KGHK}]^{2+/+}$	dsDNA	491 000	ascorbate + H_2O_2	pH 7.4, 37 °C	<i>a</i>
$[\text{Cu-KGHK}]^{2+/+}$	dsDNA	5 580	ascorbate	pH 7.4, 37 °C	18
$[\text{Cu-GGH}]^{0-}$	dsDNA	542 000	ascorbate + H_2O_2	pH 7.4, 37 °C	<i>a</i>
$[\text{Cu-GGH}]^{0-}$	dsDNA	2 340	ascorbate	pH 7.4, 37 °C	18
$[\text{Cu-neamine}]^{4+}$	dsDNA	7 690 ^b	none	pH 7.3, 37 °C	25
$[\text{Co-cyclen}]^{(4-5)+}$	dsDNA	13–90 ^b	none	pH 7.0, 37 °C	56
Eu^{3+}	dsDNA	108 ^b	none	pH 7.0, 37 °C	62
$[\text{Rh}(\text{phi})_2\text{bpy}'\text{-peptide}(\text{Zn})^0$	dsDNA	300	none	pH 6.0, 37 °C	11
$[\text{Co-tamen}]^{3+}$	dsDNA	3	none	pH 7.6, 37 °C	63
$[\text{Ce}_2\text{-HXTA}]^{3+}$	ssDNA	840	none	pH 8.0, 37 °C	64
$[\text{Ce}_2\text{-HXTA}]^{3+}$	dsDNA	78	none	pH 8.0, 37 °C	64

^aThis work. ^bEnzyme-like second-order rate constants expressed as $k_{\text{cat}}/K_{\text{M}}$.

was most likely mediated by a combination of metal-bound hydroxyl radicals and diffusible hydroxyl radicals produced in close proximity to the DNA. Although $\text{Cu}^{2+}(\text{aq})$ was observed to quickly generate diffusible hydroxyl radicals when reacted with H_2O_2 , DNA cleavage by $\text{Cu}^{2+}(\text{aq})$ was only weakly inhibited by DMSO, and linearization and nicking occurred by a notably concerted mechanism. DNA cleavage by Fe-EDTA, Fe-NTA, and Fe-TACN was most likely mediated by diffusible hydroxyl radicals produced in close proximity to the DNA, which is supported by the observation that hydroxyl radicals were produced when either Fe-NTA, Fe-EDTA, or Fe-TACN was reacted with H_2O_2 . DMSO was found to more strongly inhibit DNA cleavage by Fe-NTA and Fe-EDTA than cleavage by $\text{Cu}^{2+}(\text{aq})$ or Fe-TACN, while DNA linearization by Fe-NTA, Fe-EDTA, and Fe-TACN was less concerted than linearization by $\text{Cu}^{2+}(\text{aq})$. Previous studies have indeed shown that Fe-EDTA cleaves DNA by generation of diffusible hydroxyl radicals, but also that Fe-EDTA demonstrates subtle sequence variability in its DNA reactivity, which could be a result of weak binding sites.¹² Cu-GGH most likely functions by a similar mechanism, although the weaker DMSO inhibition of DNA cleavage by Cu-GGH suggests the primary involvement of a metal-bound hydroxyl radical in the observed DNA cleavage. Previous work has shown both that H_2O_2 is an obligatory intermediate in Cu-GGH-mediated DNA cleavage by ascorbate/ O_2 and that DMSO inhibition studies yielded no evidence of significant involvement of diffusible hydroxyl radicals in DNA cleavage, all of which is consistent with the results presented herein.¹⁸ DNA cleavage by Cu-NTA and Co-KGHK appeared to be mediated by metal-bound superoxide radicals, which is supported by the observed consumption of ascorbate when reacted with O_2 (but not H_2O_2), the apparent lack of diffusible radicals, the weak DMSO inhibition of DNA cleavage, and the concertedness of DNA linearization. DMSO inhibition profiles suggest that Ni-DOTA, Cu-EDTA, and Cu-KGHK each cleaved DNA primarily by metal-bound ROS, although no other reactivity was observed by these complexes. Freifelder–Trumbo analysis suggests that the DNA cleavage observed for $\text{Fe}^{2+}(\text{aq})$, Cu-cyclam, Cu-cyclen, Co-cyclen, Cu-EDTA, Ni-EDTA, Co-EDTA, Cu-GGH, and Co-NTA was not associated with any

binding interaction between M-chelate and DNA ($n_2/n_1 < 0.01$), while other reactive complexes (summarized in Table 2) that promoted DNA cleavage did appear to linearize DNA through a concerted mechanism ($n_2/n_1 > 0.01$). Indeed, previous studies of Cu-GGH and Cu-KGHK indicated that Cu-KGHK promoted linearization of DNA by a concerted mechanism, while Cu-GGH did not, and this most likely reflects the overall 1+ charge of Cu-KGHK and 1– charge of Cu-GGH.¹⁸ As expected, free $\text{Cu}^{2+}(\text{aq})$ and $[\text{Co-KGHK}]^+$, two of the most positively charged complexes, showed the strongest interaction with DNA as judged by n_2/n_1 values.

To compare the DNA nuclease activity of the catalysts studied herein, relative to that of other catalytic nucleases, second-order rate constants for DNA nicking reactions were established by use of eq 7, where k_{obs} is the observed first-order rate constant for DNA nicking (after subtraction of the observed background rate constant obtained in the absence of any M-chelate), and $[\text{M}]$ is the concentration of M-chelate (10^{-7} M). Table 4 compares several second-order rate constants obtained from this study with those of several other catalysts known to cleave dsDNA. Significantly higher rates were observed for several of the M-chelates studied herein.

$$k_{2,\text{nick}} = k_{\text{obs}}/[\text{M}] \quad (7)$$

CONCLUSIONS

The goal of this study was to elucidate the reactivity patterns and mechanisms of several families of metal-chelate complexes commonly incorporated in artificial nucleases. The metal-chelate complexes studied in this work were found to provide a wide range of reactivity with both co-reactants and DNA, and this reactivity was highly dependent upon several factors including reduction potential, coordination unsaturation, charge, the ability of the metal complexes to facilitate generation of ROS, and the degree to which these ROS were either metal-coordinated or diffusible. Knowledge of these factors should allow more precise tuning of gene-targeting artificial nucleases in which metal-chelates are coupled with a gene-specific targeting sequence. The degree to which the metal-chelates from this study selectively utilize biologically available co-reactants is of critical importance in

drug development, since co-reactants such as O₂, H₂O₂, and ascorbate are present at widely variable concentrations in host cells, and therefore each metal-chelate might possess differing modes of reactivity depending on such factors as location within the cell (nucleus *vs* cytoplasm) or the state of the host cell (oxidative stress *vs* normal conditions). Knowledge of the fate of the ROS produced (diffusible or metal-bound) and mechanisms of DNA cleavage for each metal-chelate is also of critical importance in the context of gene targeting, because those metal-chelates which generate an excess of diffusible radicals will likely be less selective toward a targeted gene, with the possibility of damage to non-targeted genes, while the metal-chelates that cleave DNA by more controlled means, such as through metal-bound ROS, will more likely be selective toward the targeted gene. In this study we found that several metal-chelates (Cu-cyclen, Ni-DOTA, Cu-EDTA, Cu-GGH, Co-KGHK, Cu-KGHK, and Cu-NTA) appear to cleave DNA primarily by metal-bound ROS rather than diffusible ROS, and therefore, incorporation of these metal complexes in artificial nucleases should provide more controlled delivery of ROS to targeted genes. Finally, many of the metal-chelates from this study possess desirable therapeutic properties, such as the ability to perform multiple turnovers or efficiently utilize biologically available co-reactants. Compounds that alter biological targets irreversibly and with multiple turnovers, such as these metal-chelates, have the potential to perform at far lower concentrations than their reversible counterparts, since catalytic drugs that promote irreversible inactivation of a target do not need to saturate the target in order to operate effectively.^{15,16,18,19,25} Lower dosage concentrations should result in fewer side effects and higher efficacy.

■ ASSOCIATED CONTENT

S Supporting Information. O₂ dependence of ascorbate consumption; kinetic traces for the ascorbate consumption, TEMPO-9-AC, and rhodamine B reactions; summary of rhodamine B initial reaction rates; square-wave voltammogram; structures and reaction mechanisms for TEMPO-9-AC and rhodamine B; summary of DNA nicking and linearization rate constants; and complete ref 8. This material is available free of charge via the Internet at <http://pubs.acs.org>.

■ AUTHOR INFORMATION

Corresponding Author

cowan@chemistry.ohio-state.edu

■ ACKNOWLEDGMENT

This work was supported by grants from the National Institutes of Health (HL093446 and AA016712). J.C.J. was supported by an NIH Chemistry/Biology Interface training grant (T32 GM08512).

■ REFERENCES

- (1) Cowan, J. A. *Inorganic Biochemistry. An Introduction*; Wiley-VCH: New York, 1997; pp 342–345.
- (2) Reedijk, J. *Med. Inorg. Chem.* **2005**, 80–109.
- (3) Liu, H.-K.; Sadler, P. J. *Acc. Chem. Res.* **2011**, 44, 349–359.
- (4) Wheate, N. J.; Brodie, C. R.; Collins, J. G.; Kemp, S.; Aldrich-Wright, J. R. *Mini Rev. Med. Chem.* **2007**, 7, 627–48.
- (5) Boger, D. L.; Garbaccio, R. M. *Acc. Chem. Res.* **1999**, 32, 1043–1052.

- (6) Minoshima, M.; Bando, T.; Shinohara, K.; Sugiyama, H. *Nucleic Acids Symp. Ser.* **2009**, 53, 69–70.
- (7) Baum, C.; von Kalle, C.; Staal, F.; Li, X.; Fehse, B.; Schmidt, M.; Weerkamp, F.; Karlsson, S.; Wagemaker, G.; Williams, D. *Molec. Ther.* **2004**, 9, 5–13.
- (8) Hacein-Bey-Abina, S.; et al. *Science* **2003**, 302, 415–419.
- (9) Magda, D.; Wright, M.; Crofts, S.; Lin, A.; Sessler, J. J. *Am. Chem. Soc.* **1997**, 119, 6947–6948.
- (10) Dreyer, G.; Dervan, P. *Proc. Natl. Acad. Sci. U.S.A.* **1985**, 82, 968–972.
- (11) Fitzsimons, M. P.; Barton, J. K. *J. Am. Chem. Soc.* **1997**, 119, 3379–3380.
- (12) Sigman, D. *Biochemistry* **1990**, 29, 9097–9105.
- (13) Sigman, D.; Bruice, T.; Mazumder, A.; Sutton, C. *Acc. Chem. Res.* **1993**, 26, 98–104.
- (14) Dervan, P. *Science* **1986**, 232, 464–471.
- (15) Hocharoen, L.; Cowan, J. A. *Chem.—Eur. J.* **2009**, 15, 8670–8676.
- (16) Jin, Y.; Cowan, J. A. *J. Am. Chem. Soc.* **2006**, 128, 410–411.
- (17) Jin, Y.; Cowan, J. A. *J. Biol. Inorg. Chem.* **2007**, 12, 637–644.
- (18) Jin, Y.; Cowan, J. A. *J. Am. Chem. Soc.* **2005**, 127, 8408–8415.
- (19) Cowan, J. A. *Pure Appl. Chem.* **2008**, 80, 1799–1810.
- (20) Jin, Y.; Lewis, M. A.; Gokhale, N. H.; Long, E. C.; Cowan, J. A. *J. Am. Chem. Soc.* **2007**, 129, 8353–8361.
- (21) Bradford, S.; Kawarasaki, Y.; Cowan, J. A. *J. Inorg. Biochem.* **2009**, 103, 871–875.
- (22) Silver, G. C.; Troglor, W. C. *J. Am. Chem. Soc.* **1995**, 117, 3983–3993.
- (23) Cooke, M.; Evans, M.; Dizdaroglu, M.; Lunec, J. *FASEB J.* **2003**, 1195–1214.
- (24) Inoue, S.; Kawanishi, S. *Canc. Res.* **1987**, 47, 6522–6527.
- (25) Sreedhara, A.; Freed, J. D.; Cowan, J. A. *J. Am. Chem. Soc.* **2000**, 122, 8814–8824.
- (26) Long, E. C. *Acc. Chem. Res.* **1999**, 32, 827–836.
- (27) Ogino, H.; Ogino, K. *Inorg. Chem.* **1982**, 22, 2208–2211.
- (28) Henle, E. S.; Han, Z.; Tang, N.; Rai, P.; Luo, Y.; Linn, S. *J. Biol. Chem.* **1999**, 274, 962–971.
- (29) Pogozelski, W.; Tullius, T. *Chem. Rev.* **1998**, 98, 1089–1107.
- (30) Chiou, S.-H. *J. Biochem.* **1984**, 96, 1307–1310.
- (31) Camerman, N.; Camerman, A.; Sarkar, B. *Can. J. Chem.* **1976**, 54, 1309–1316.
- (32) Finnen, D.; Pinkerton, A.; Dunham, W.; Sands, R.; Funk, M. *Inorg. Chem.* **1990**, 30, 3960–3964.
- (33) Viola-Villegas, N.; Doyle, R. *Coord. Chem. Rev.* **2009**, 253, 1906–1925.
- (34) Mizuta, T.; Wang, J.; Miyoshi, K. *Inorg. Chim. Acta* **1995**, 230, 119–125.
- (35) Walters, M. A.; Vapnyar, V.; Bolour, A.; Incarvito, C.; Rheingold, A. L. *Polyhedron* **2003**, 22, 941–946.
- (36) Ren, Y.-W.; Li, J.; Zhao, S.-M.; Zhang, F.-X. *Struct. Chem.* **2004**, 16, 439–444.
- (37) Cernak, J.; Kuchar, J.; Stolarova, M.; Kajnakova, M.; Vavra, M.; Potocnak, I.; Falvello, L. R.; Tomas, M. *Trans. Met. Chem.* **2010**, 35, 737–744.
- (38) Freifelder, D.; Trumbo, B. *Biopolymers* **1969**, 7, 681–693.
- (39) Joyner, J. C.; Cowan, J. A. *J. Am. Chem. Soc.* **2011**, 133, 9912–9922.
- (40) Pou, S.; Bhan, A.; Bhadti, V. S.; Wu, S. Y.; Hosmane, R. S.; Rosen, G. M. *FASEB J.* **1995**, 9, 1085–1090.
- (41) Matko, J.; Ohki, K.; Edidin, M. *Biochemistry* **1992**, 31, 703–711.
- (42) Cohn, C. A.; Simon, S. R.; Schoonen, M. A. *Part. Fibre Toxicol.* **2008**, 5, 2.
- (43) Laight, D. W.; Andrews, T. J.; Haj-Yehia, A. I.; Carrier, M. J.; Ånggård, E. E. *Environ. Toxicol. Pharmacol.* **1997**, 3, 65–68.
- (44) Samuni, A.; Goldstein, S.; Russo, A.; Mitchell, J. B.; Krishna, M. C.; Neta, P. *J. Am. Chem. Soc.* **2002**, 124, 8719–8724.
- (45) Yu, F.; Xu, D.; Lei, R.; Li, N.; Li, K. *J. Agric. Food Chem.* **2008**, 13, 730–735.

- (46) Mishra, K. P.; Gogate, P. R. *Sep. Purif. Technol.* **2010**, *75*, 385–391.
- (47) Wood, P. *Biochem. J.* **1988**, *253*, 287–289.
- (48) Borsook, H.; Keighley, G. *Proc. Natl. Acad. Sci. U.S.A.* **1933**, *19*, 875–878.
- (49) Lau, S.-J.; Sarkar, B. *J. Biol. Chem.* **1971**, *246*, 5938–5943.
- (50) Lau, S.-J.; Kruck, T. P. A.; Sarkar, B. *J. Biol. Chem.* **1974**, *249*, 5878–5884.
- (51) Grogan, J.; McKnight, C. J.; Troxler, R. F.; Oppenheim, F. G. *FEBS Lett.* **2001**, *491*, 76–80.
- (52) Cabras, T.; Patamia, M.; Melino, S.; Inzitari, R.; Messina, L.; Castagnola, M.; Petruzzelli, R. *Biochem. Biophys. Res. Commun.* **2007**, *358*, 277–284.
- (53) Bradshaw, R. A.; Peters, T. *J. Biol. Chem.* **1969**, *244*, 5582–5589.
- (54) Buettner, G. R.; Jurkiewicz, B. A. *Radiat. Res.* **1996**, *145*, 532–541.
- (55) Jeung, C.-S.; Kim, C. H.; Min, K.; Suha, S. W.; Suha, J. *Bioorg. Med. Chem. Lett.* **2001**, *11*, 2401–2404.
- (56) Hettich, R.; Schneider, H. J. *J. Am. Chem. Soc.* **1997**, *119*, 5638.
- (57) Barrette, W. C. J.; Sawyer, D. T.; Fee, J. A.; Asada, K. *Biochemistry* **1983**, *22*, 624–627.
- (58) Azab, H. A.; Banci, L.; Borsari, M.; Luchinat, C.; Sola, M.; Viezzoli, M. S. *Inorg. Chem.* **1992**, *31*, 4649–4655.
- (59) Tullius, T. D.; Dombroski, B. A. *Proc. Natl. Acad. Sci. U.S.A.* **1986**, *83*, 5469–5473.
- (60) Sagripanti, J.-L.; Goering, P. L.; Lamanna, A. *Toxicol. Appl. Pharmacol.* **1991**, *110*, 477–485.
- (61) Huang, X.; Pieczko, M. E.; Long, E. C. *Biochemistry* **1999**, *38*, 2160–2166.
- (62) Rammo, J.; Hettich, R.; Roigk, A.; Schneider, H. J. *Chem. Commun.* **1996**, 105.
- (63) Dixon, N. E.; Geue, R. J.; Lambert, J. N.; Moghaddas, S.; Pearce, D. A.; Sargeson, A. M. *Chem. Commun.* **1996**, 1287–1288.
- (64) Branum, M. E.; Tipton, A. K.; Zhu, S.; Que, L. J. *J. Am. Chem. Soc.* **2001**, *123*, 1898.